Table 1 Summary of frequency content

Time, s	F1, Hz	F2, Hz	F3, Hz	Spin, Hz	$\dot{\phi}_1$,[a] Hz	$\dot{\phi}_1$,[a] Hz
			Round 43			
4.09	72.5	78.5[b]	ne[c]	78.4	...	1.0
10.24	70.3	↑	ne	76.5	6.5	1.4
16.38	68.5		ne	74.5	8.0	1.5
21.50	67.3		ne	73.3	...	...
26.60	66.3	71.0	ne	...	...	...
		↑				
			Round 44			
2.04	73.5	79.2	ne	80.3	...	1.0
5.00	72.5	↑	ne	79.1	...	...
10.10	70.6		ne	77.2	7.0	1.4
15.20	69.4		ne	75.5	6.5	1.5
19.09	68.3	73.6	ne	74.5	6.0	1.4
		↑				
			Round 45			
1.02	71.3	76.6	ne	84.0	...	...
8.18	71.0	↑	ne	77.2	...	...
13.30	69.4		5.6	75.0	...	...
17.40	68.2		5.8	73.5	...	...
22.52	66.8		ne	...	...	...
25.59	66.2		ne	...	...	...
28.67	65.2	70.5	ne	...	...	...
			Round 47			
2.04	80.9	4.9	ne	80.3	6.5	1.0
5.11	79.4	4.8	ne	79.4	7.0	1.0
11.26	78.0	5.1	ne	77.4	7.0	1.5
17.40	76.1	4.9	ne	75.4	6.5	1.6
23.55	74.2	5.0	ne	...	...	...
28.67	72.5	5.0	ne	...	...	...

[a] Estimated from yawsonde data.
[b] Numerical entries joined by lines indicate a range of estimated values.
[c] Not strongly evident within the reduced data.

44, and 45, the F2 frequency component is approximately equal to p or $p-\dot{\phi}_2$. The F1 frequency response, however, closely follows $p-\dot{\phi}_1$. The measurement of a strain frequency, say s, is, of course, made onboard the spinning projectile. This frequency, when viewed in terms of an Earth-fixed coordinate system becomes $p-s$. Hence, we expect that the fundamental responses of the strain gage bridge will be $p-\dot{\phi}_1$ and $p-\dot{\phi}_2$. The frequency resolution is not sufficiently accurate to distinguish between a response of p or $p-\dot{\phi}_2$, but the actual response frequency is $p-\dot{\phi}_2$. Note that although the yawing motion is essentially steady, the spin is decreasing due to aerodynamic roll damping. Therefore, we expect $p-\dot{\phi}_1$ to decrease with time; $\dot{\phi}_1$ also varies with time, but normally not as fast as p. The variation in $p-\dot{\phi}_1$ is primarily due to the decrease in p.

The behavior observed for round 47, Fig. 3, was unlike the three other rounds and was quite unusual. This may have been expected since the liquid payloads in rounds 43, 44, and 45 were similar, but round 47 was not. The F1 component closely follows $p-\dot{\phi}_2$ and not $p-\dot{\phi}_1$, while the F2 component is approximately 5 Hz. The three other rounds had an intermittent or very weak response in the 5 Hz range. Within Table 1, the F2 response of round 47 was tracked at a very steady value of 5 Hz. This response could be produced by the liquid payload. It is also possible that this F2 response is produced by some mechanism not asociated with the liquid, perhaps the canisters which are separately keyed to the projectile body. From Table 1, the F2 response seems to follow a beat frequency of $(\dot{\phi}_1-\dot{\phi}_2)$, but there is good agreement only at the 17.4 s time frame. It is not clear from physical considerations that F2 is related to $\dot{\phi}_1-\dot{\phi}_2$, and the flight data do not strongly suggest such a conclusion. At present, the origin of the F2 response for round 47 was not produced by the yawing motion, which from the yawsonde data was damped. This type of response could provide a resonance mechanism with a fuze. In particular, a common fuze used on this projectile has a mechanical timer with an escapement mechanism that oscillates at 80 Hz.

In-flight measurements of strain and the associated vibrations in the vicinity of the ogive of spin-stabilized projectiles were made. A vibration history of one liquid-carrying projectile was quite unusual. For this projectile, a frequency component equal to the difference between the spin frequency and the precessional frequency was observed. The amplitude of this component increased dramatically in the second half of the trajectory, while the associated yawing motion measured in that region of the trajectory was quite stable. This suggests that the energy associated with these vibrations was growing, but the vibrations were not large enough to modify the motion of the projectile.

References

[1] D'Amico, W.P., "An Investigation of the Flight Vibration Environment of the 155 mm M687-IVA Projectile," BRL Memo. Rept. 2755, AD B0197920, U.S. Army Ballistic Research Laboratory, Aberdeen Proving Ground, Md., June 1977.

[2] D'Amico, W.P., "In-Flight Measurements of Vibrations for the XM736 Binary Projectile," BRL Memo. Rept. 2793, AD B0249540, U.S. Army Ballistic Research Laboratory, Aberdeen Proving Ground, Md., Sept. 1977.

[3] Whyte, R.H. and Mermagen, W.H., "A Method for Obtaining Aerodynamic Coefficients from Yawsonde and Radar Data," AIAA Paper 72-978, AIAA 2nd Atmospheric Flight Mechanics Conference, Palo Alto, Calif., Sept. 1972.

[4] Murphy, C.H., "Effect of Large High-Frequency Angular Motion of a Shell on the Analysis of Its Yawsonde Records," BRL Memo. Rept. 2581, AD B0094210, U.S. Army Ballistic Research Laboratory, Aberdeen Proving Ground, Md., Feb. 1976.

Melting of Solid Bodies Due to Convective Heating with the Removal of Melt

Anant Prasad*
Regional Institute of Technology, Jamshedpur, India

Nomenclature

c = heat capacity per unit volume of the material
D = thermal dissipation
h = heat transfer coefficient
H = heat flow vector
k = thermal conductivity of the material
L = latent heat of the material
m = dimensionless thickness of the melt removal $= hq_3/k$
$q_1(t)$ = unknown surface temperature
$q_2(t)$ = unknown penetration depth
$q_3(t)$ = unknown thickness of melt removal
Q = thermal force
S_t = inverse of Stefan number $= \rho L/cT_m$
t = time
T = temperature
V = thermal potential
x = direction in which heat is applied

Received Feb. 13, 1979; revision received May 7, 1979.

Index categories: Heat Conduction; Ablation, Pyrolysis, Thermal Decomposition and Degradation (including Refractories).

*Assistant Professor, Dept. of Mechanical Engineering.

α = thermal diffusivity of the material
η = dimensionless penetration depth = hq_2/k
θ = dimensionless temperature = T/T_m
ρ = density of the material
τ = dimensionless time = h^2t/kc

Subscripts

a = condition of the surroundings
i = initial condition
m = condition at initiation of melting
s = steady-state condition

Introduction

HEATING and melting of ablating materials with the removal of melt due to convective or aerodynamic heating is of great significance in the design of protective layers of missiles and space vehicles. It is a phase change problem involving nonlinearity as a result of the moving boundary in the mathematical model and it is not possible to find its solution by exact analyses unless a finite-difference method is employed. This takes much computer time and the numerical results are restricted to those values of parameters for which they are calculated. To overcome such a difficulty, Biot's variational principle,[1] an approximate analytical method, has been used in a number of phase change problems by several investigators.[2-9] The phase change occurred due to melting of solids and the melt was not removed. Biot and Daughaday[10] considered this problem with the removal of melt for uniform heat flux. The thermophysical properties were assumed to be constant and the solid was initially at its melting temperature. It was later solved by Biot and Agrawal[11] using temperature-dependent thermophysical properties.

In the present analysis, the problem is studied where melting of the solid occurs due to convective heating and the melt is removed as soon as it is formed on the surface of the solid. The assumption that the solid is at its melting temperature is removed in order to account for the heating regime preceding melting. For both regimes, solutions are obtained in closed form. Numerical solutions are also found.

Mathematical Model

A semi-infinite solid of constant cross-sectional area subjected to one-dimensional convective heating is considered. It is initially at a uniform temperature T_i which is less than the melting temperature of the solid. After time t from the initiation of heating, $q_1(t)$ and $q_2(t)$ represent, respectively, the temperature buildup at the surface and the thermal penetration depth. With increase in time, both increase and eventually $q_1(t)$ reaches the melting temperature T_m of the solid. The corresponding penetration depth becomes $q_{2m}(t)$. Assuming the thermophysical properties of the solid to be uniform, the equation governing heat transfer during the premelting heating regime ($0<t\leq t_m$) in terms of dimensionless variables is

$$\partial^2\theta/\partial^2\xi = \partial\theta/\partial\tau \qquad (\xi>0,\ 0<\tau\leq\tau_m) \tag{1}$$

The related dimensionless initial and boundary conditions are

$$\theta=\theta_i \qquad \eta=0 \qquad (\tau=0) \tag{2}$$

$$\partial\theta/\partial\xi=\theta_1-\theta_a \qquad (\xi=0,\ 0<\tau\leq\tau_m,\ \theta_a>\theta_1) \tag{3}$$

$$\partial\theta/\partial\xi=0 \quad \theta=\theta_i \qquad (\xi=\eta,\ 0<\tau\leq\tau_m) \tag{4}$$

where $\xi = hx/k$.

When heating of the solid is continued for time t greater than the time for the surface to reach the melting temperature ($t>t_m$), melting occurs and the melt is removed as soon as it is formed on the surface. If $q_3(t)$ is the distance of the melt removed at any time t ($t>t_m$) and during melting $q_2(t)$ denotes the penetration depth measured from the new surface formed for the heating after removal of the melt $q_3(t)$, the nondimensional equation describing heat transfer in the solid takes the form

$$\partial^2\theta/\partial\xi^2 = \partial\theta/\partial\tau \qquad (\xi>m,\quad \tau>\tau_m) \tag{5}$$

In this regime, the thermophysical properties of the solid are taken to be constant. The nondimensional initial and boundary conditions for Eq. (5) are

$$\theta=1,\ m=0 \qquad \eta=\eta_m \qquad \tau=\tau_m \tag{6}$$

$$\theta=\theta_i \qquad \xi=\eta_m \qquad \tau=\tau_m \tag{7}$$

$$\theta=1 \qquad \xi=m \qquad \tau>\tau_m \tag{8}$$

$$\partial\theta/\partial\xi=0 \qquad \xi=\eta+m \qquad \tau>\tau_m \tag{9}$$

whereas in the melting process

$$(\theta_a-1)=[(1-\theta_i)+S_t]\,\mathrm{d}m/\mathrm{d}t+\mathrm{d}H^*/\mathrm{d}t \qquad \xi=m \qquad \tau>\tau_m \tag{10}$$

Equation (10) states that the heat supplied by convective heating is equal to the heat taken to melt the solid to a depth m and to raise the temperature of this depth from its initial temperature to the melting temperature and the heat penetration to the depth η measured from the newly formed surface.

Solution

In order to apply Biot's variational principle to obtain solutions for both regimes, a temperture distribution of cubic profile, which yielded reliable results in earlier investigations,[10,11] is assumed in the solid

$$\theta-\theta_i=(\theta_1-\theta_i)\,[1-(\xi-m)/\eta]^3 \tag{11}$$

Here, θ_1 is the surface temperature; η and m are, respectively, the penetration depth and the depth of melt removal. They are unknown generalized coordinates to be determined as functions of time. In the premelting heating regime, the surface temperature increases with time but does not exceed the melting temperature of the solid. As a result there is no formation of melt ($m=0$). When they are employed in Eq. (11), it gives the temperature distribution in this regime whereas the penetration depth of this equation represents the depth from the surface $\xi=0$. For the melting and melt removal regime, the surface temperature θ_1 in Eq. (11) stands for the temperature of the newly formed surface after removal of melt to the depth m. This surface remains always at the melting temperature of the solid and the penetration depth is measured from the new surface.

In nondimensional form, the conservation of energy may be written as

$$\mathrm{Div}H^* = -(\theta-\theta_i) \tag{12}$$

where $H=kcT_mH^*h$. Using Eqs. (11) and (12), the heat flowfield becomes

$$H^*=\tfrac{1}{4}\eta(\theta_1-\theta_i)\,[1-(\xi-m)/\eta]^4 \tag{13}$$

This equation satisfies the boundary condition [Eq. (4)] in the premelting heating regime and Eq. (9) in the melting and melt removal regime.

Knowing the temperature field and heat flowfield, the Lagrangian equation based on Biot's variational principle is applied.

$$\partial V^*/\partial\eta + \partial D^*/\partial\dot{\eta} = Q^* \tag{14}$$

In this equation, V^* is the nondimensional themal potential, D^* the nondimensional thermal dissipation, and Q^* the nondimensional thermal force. They are expressed, respectively,

$$V^* = hV/kcT_m^2 = \tfrac{1}{2}\int_m^{\eta+m} (\theta-\theta_i)^2 \mathrm{d}\eta \tag{15}$$

$$D^* = D/hT_m^2 = \tfrac{1}{2}\int_m^{\eta+m} (\mathrm{d}H^*/\mathrm{d}t)^2 \mathrm{d}\eta \tag{16}$$

$$Q^* = Q/cT_m^2 = [(\theta-\theta_i)(\partial H^*/\partial\eta)]_{\xi=m} \tag{17}$$

Employing Eqs. (11) and (13), the Lagrangian equation [Eq. (14)] in the unknown generalized coordinate η reduces to

$$\eta[(4/112)\dot{\eta}(\theta_1-\theta_i)^2 + (11/112)\dot{m}(\theta_1-\theta_i)^2 + (3/144)\eta\dot{\theta}_1(\theta_1-\theta_i)] = (5/14)(\theta_1-\theta_i)^2 \tag{18}$$

A. Premelting Heating Regime ($\tau \le \tau_m, \eta \le \eta_m, \theta_1 \le 1$)

In this regime, $m = \dot{m} = 0$; θ_1 is time dependent and less than the melting temperature of the solid. They reduce Eq. (18) to

$$4\eta[(9/8)\dot{\eta}(\theta_1-\theta_i) + (21/32)\eta\dot{\theta}_1] = 45(\theta_1-\theta_i) \tag{19}$$

A second relationship between these two generalized coordinates η and θ_1 can be provided by combining Eqs. (3) and (11):

$$\eta = 3(\theta_1-\theta_i)/(\theta_a-\theta_1) \tag{20}$$

In this equation, m is taken to be zero and it is noted that such a relationship has been used in earlier studies.[3,4] When the surface attains the melting temperature of the solid ($\theta_1 = 1$), this equation gives an expression for the penetration depth

$$\eta = \eta_m = 3(1-\theta_i)/(\theta_a-1) \tag{21}$$

Eliminating η from Eqs. (19) and (20) gives an equation for surface temperature

$$\dot{\theta}_1 = (40/63)(\theta_a-\theta_1)^3/(\theta_1-\theta_i)[(57/63)(\theta_a-\theta_1) + (36/63)(\theta_1-\theta_i)] \tag{22}$$

To obtain the surface temperature time history, Eq. (22) is solved using Simpson's numerical integration formula. The limit of intergration is taken from θ_i to 1. Its closed-form solution is also found.

$$\tau = A_0[A_1/(\theta_a-\theta_1)^2 - A_2/(\theta_a-\theta_1) + A_3 \ln(\theta_a-\theta_1)/(\theta_a-\theta_i) - A_4] \tag{23}$$

where

$$A_0 = 63/40 \quad A_1 = (18/63)(\theta_a-\theta_i)^2 \quad A_2 = (15/63)(\theta_a-\theta_i) \quad A_3 = 21/63 \quad A_4 = 1/21$$

It satisfies the initial condition [Eq. (2)].

B. Melting and Melt Removal Regime ($\tau > \tau_m$, $\eta > \eta_m$, $\theta_1 = 1$)

Here, $\theta_1 = 1$, $\dot{\theta}_1 = 0$, and m is a function of time. When they are employed in the Lagrangian equation [Eq. (18)], it becomes

$$280 = \eta(28\dot{\eta} + 77\dot{m}) \tag{24}$$

This gives a relationship between two unknown generalized coordinates η and m. An auxiliary equation,[1,10,11] which relates them, is obtained using Eqs. (10) and (13)

$$(\theta_a-1) = [(1-\theta_i) + S_t)]\dot{m} + \tfrac{1}{4}(1-\theta_i)\dot{\eta} \tag{25}$$

Combination of Eqs. (24) and (25) gives

$$C_1 = C_2\eta\dot{\eta} + C_3\eta \tag{26}$$

$$-C_6 = C_4\eta\dot{m} - C_5\eta \tag{27}$$

where

$$C_1 = 280[(1-\theta_i) + S_t] \quad C_2 = [35(1-\theta_i) + 112S_t]/4$$
$$C_3 = 77(\theta_a-1) \quad C_4 = 4C_2 \quad C_5 = 112(\theta_a-1) \quad C_6 = 280(1-\theta_i)$$

It is noted that this method reduces the nonlinear problem to an initial value problem giving a pair of ordinary differential equations [Eqs. (26) and (27)] with the independent variable time. A closed-form solution for Eq. (26) is

$$\tau = \tau_m + (C_2/C_3)(\eta_m-\eta) + (C_1C_2/C_3^2)\ln(C_1-C_3\eta_m)/(C_1-C_3\eta) \tag{28}$$

which satisfies the initial condition [Eq. (6)] Next, combination of Eqs. (26) and (27) gives

$$\dot{m}/\dot{\eta} = \mathrm{d}m/\mathrm{d}\eta = (C_5\eta - C_6)/(C_1-C_3\eta) \tag{29}$$

Its solution in terms of penetration depth η is

$$m = B_1(\eta_m-\eta) + B_2\ln(C_1-C_3\eta_m)/(C_1-C_3\eta) \tag{30}$$

where

$$B_1 = C_2C_5/C_4C_3 \qquad B_2 = C_2(C_3C_6 - C_1C_5)/C_4C_3^2$$

In this regime, the maximum penetration depth is determined from the fact that $\dot{\eta} = 0$. Substituting this in Eq. (26) gives

$$\eta = \eta_s = C_1/C_3 \tag{31}$$

It is the maximum value as it fulfills the condition $\mathrm{d}^2\eta/\mathrm{d}\tau^2 = 0$. It is called the steady-state penetration depth because the time rate of penetration $\dot{\eta}$ does not assume a negative value after this condition has been reached. The corresponding melt removal can be obtained employing Eq. (31) in Eq. (30).

Results and Discussion

To study the behavior of temperature buildup θ_1, thermal penetration depth η, and melt removal m, they are displayed in Fig. 1. It consists of two regimes. Regime I is the heating regime where melting is absent and according to Eqs. (20) and (22), they are dependent on the initial temperature of the solids θ_i and the surrounding temperature θ_a. Their typical values are taken as 0.1 and 1.3, respectively, in plotting the graphs in Fig. 1. It is seen that in the initial period of heating the penetration depth η increases very rapidly with the corresponding rapid buildup of surface temperature θ_1. With a further elapse of time, both of them increase slowly, and when the surface attains the melting temperature of the solid, the penetration depth approaches a value 9 which can be obtained employing Eqs. (21).

In Fig. 2, these results are compared with the results of exact analysis[12] and Goodman's approximate analysis based on the heat balance integral method.[13] It is observed that there is close agreement. However, the present method

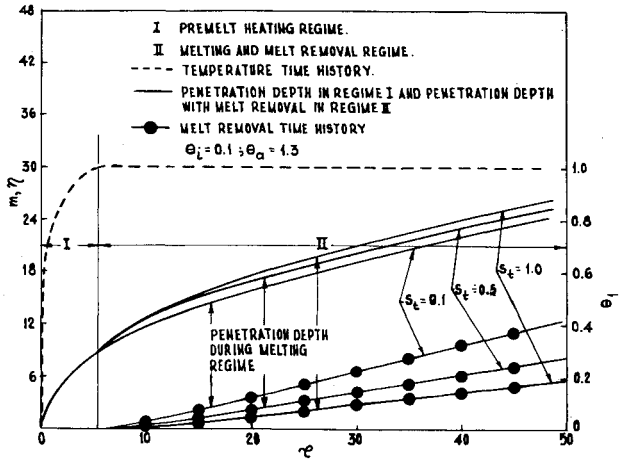

Fig. 1 Behavior of temperature buildup θ_1, thermal penetration depth η, and melt removal m with time for different values of S_t taken as a parameter.

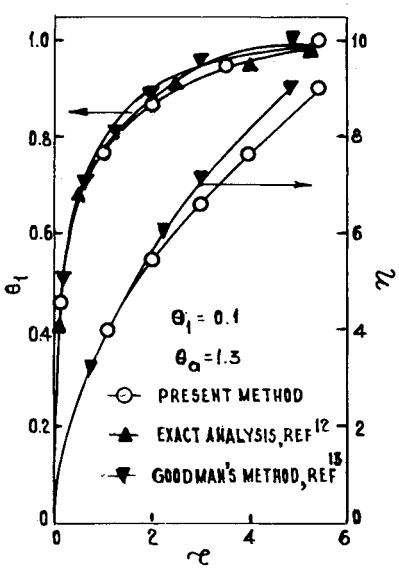

Fig. 2 Comparison of temperature buildup time history and thermal penetration depth time history in the premelt heating regime with available results.

predicts better results as it overestimates by 2.4% the time for the surface to attain the melting temperature of the solid in comparison with Goodman's method which underestimates it by 8.5%. In both methods, a cubic temperature profile is used. The relation between penetration depth and temperature buildup at the surface [Eq. (20)] obtained by the present method is the same as that found employing Goodman's method.

Regime II represents the melting and melt removal regime and is controlled by the inverse of the Stefan number S_t. In Fig. 1, melt removal time history and penetration depth time history are shown with S_t as a parameter. The values of S_t are realistic for ablating materials.[14] For each value of S_t, both η and m increase rapidly near the onset of melting and m achieves a steady-state value as the penetration depth reaches its steady-state value, which can be obtained using Eq. (31). With increase in S_t, η increases at any time τ, whereas the corresponding melt removal decreases. Physically, this is true in view of the fact that at a higher S_t the solid offers less resistance to heat transmission than with a lower value of S_t. As a result the heat penetration depth is greater and less heat is available to melt the solid leading to a small value of m.

Conclusions

Heating and melting with melt removal is analyzed when a semi-infinite solid is subjected to one-dimensional convective heating. Using Biot's variational method, the mathematical complexity due to the presence of nonlinearity is reduced and a closed-form solution is obtained for both the premelt heating regime and the melting regime. In the latter regime both η and m are dependent on the inverse of the Stefan number S_t. The steady-state solution is obtained directly as the limit of the transient solutions. In the premelt heating regime, results are obtained close to those of exact analysis and a heat balance integral method.

References

[1] Biot, M.A., *Variational Principle in Heat Transfer,* Oxford University Press, London, 1970, pp. 92-95.

[2] Prasad, A. and Agrawal, H.C., "Biot's Variational Principle for a Stefan Problem," *AIAA Journal,* Vol. 10, March 1972, pp. 325-327.

[3] Prasad, A. and Agrawal, H.C., "Biot's Variational Principle for Aerodynamic Ablation of Melting Solids," *AIAA Journal,* Vol. 12, Feb. 1974, pp. 250-252.

[4] Prasad, A., "Effect of Temperature-Dependent Heat Capacity on Aerodynamic Ablation of Melting Bodies," *AIAA Journal,* Vol. 16, Sept. 1978, pp. 1004-1007.

[5] Prasad, A. and Sinha, S.N., "Radiative Ablation of Melting Solids," *AIAA Journal,* Vol. 14, Oct. 1976, pp. 1494-1497.

[6] Lardner, T.J., "Approximate Solution to Phase-Change Problems," *AIAA Journal,* Vol. 5, Nov. 1967, pp. 2079-2080.

[7] Chung, B.T.F. and Yeh, L.T., "Solidification and Melting of Materials subject to Convection and Radiation," *Journal of Spacecraft and Rockets,* Vol. 12, June 1975, pp. 329-333.

[8] Yeh, L.T. and Chung, B.T.F., "Transient Heat Conduction in a Finite Medium with Phase Change," ASME Paper 76 WA/HT-3, 1976.

[9] Yeh, L.T. and Chung, B.T.F., "Phase Change in a Radiative and Convective Medium with Variable Properties," *Journal of Spacecraft and Rockets,* Vol. 14, March 1977, pp. 178-182.

[10] Biot, M.A. and Daughaday, H., "Variational Analysis of Ablation," *Journal of Aerospace Sciences,* Vol. 29, Feb. 1962, pp. 227-229.

[11] Biot, M.A. and Agrawal, H.C., "Variational Analysis of Ablation for Variable Properties," *Transactions of ASME, Journal of Heat Transfer, Series C,* Vol. 86, 1964, pp. 437-442.

[12] Carslaw, H.S. and Jaeger, J.C., *Conduction in Solids,* Oxford University Press, N.Y., 1959, p. 72.

[13] Eckert, E.R.G. and Drake, R.M., *Analysis of Heat and Mass Transfer,"* International Student Edition, McGraw-Hill Kogakusha, Ltd., Tokyo, 1972, p. 187.

[14] Rohsenow, W.M. and Hartnett, J.P., *Handbook of Heat Transfer,* McGraw-Hill, N.Y., 1973, pp. 16-49.